Vol. 492: 21–39, 2013
doi: 10.3354/meps10468

MARINE ECOLOGY PROGRESS SERIES
Mar Ecol Prog Ser

Published October 31

Internal versus external drivers of periodic hypoxia in a coastal plain tributary estuary: the York River, Virginia

Samuel J. Lake*, Mark J. Brush, Iris C. Anderson, Howard I. Kator

Virginia Institute of Marine Science, College of William and Mary, PO Box 1346, Gloucester Point, Virginia 23062, USA

ABSTRACT: The formation of periodic hypoxia within tributary estuaries, and its relationship to the spring-neap tidal cycle, has been well documented in several systems along the US east coast. However, the importance and scale of other physical and biological processes, which ultimately control the frequency and spatial extent of hypoxia, are less well understood. This study synthesized *in situ* measurements, metabolic incubations, and high-resolution water quality monitoring into a spatially explicit, temporally integrated mass balance to examine the significance of multiple organic matter sources and oxygen sinks in relation to hypoxia in the York River estuary (YRE), Virginia, USA. Results highlight episodic peaks in gross primary production (GPP) mostly unrelated to the spring-neap cycle, with phytoplankton accounting for the bulk of total GPP. Despite extensive shoals, microphytobenthos contributed under 20% and typically under 10% of total GPP. Respiration rates were sufficient to drive bottom waters to hypoxia during transitions from spring to neap tides. While GPP generally appeared to be relatively balanced with respiration, results indicated an area at the mesohaline–polyhaline boundary that was net heterotrophic. Phytoplankton production dominated the estimated inputs of organic carbon from the tributaries and surrounding watersheds, and was 1.5 times greater than inputs from the Chesapeake Bay, which roughly balanced exports. Management efforts to alleviate hypoxia should focus on reducing internal phytoplankton production, although inputs of labile organic matter from the Chesapeake Bay represent an important source that can only be controlled by more regional efforts.

KEY WORDS: York River · Hypoxia · Production · Respiration · Net ecosystem · Metabolism · Carbon budget

INTRODUCTION

Hypoxia represents one of the most common and ecologically detrimental outcomes of anthropogenic nutrient enrichment in coastal marine ecosystems (Diaz & Rosenberg 1995, 2008). Hypoxia (defined here as ≤2.0 mg O_2 l^{-1}) and eutrophication within the Chesapeake Bay and its tributaries have been intensively studied with large-scale monitoring programs and smaller-scale high intensity sampling over the past 25 yr in response to declining water quality, increasing deep water hypoxia, and loss of submerged aquatic vegetation between the 1950s and 1980s (Cooper & Brush 1991, 1993, D'Elia et al. 2003, Kemp et al. 2005). The seasonal development of anoxia within the mainstem of the Chesapeake Bay has been linked to the input of fresh water (primarily from the Susquehanna and Potomac Rivers) and associated influx of organic matter and nutrients during high flow periods (winter and spring), the production and subsequent deposition of organic matter during the spring phytoplankton bloom, and density driven water column stratification (Taft et al. 1980, Officer et al. 1984, Seliger et

*Email: sjlake@vims.edu

al. 1985, de Jonge & van Beusekom 1995, Cloern 2001, Hagy et al. 2004, Kemp et al. 2005). Bacterial respiration of the deposited autochthonous and allochthonous organic matter fuels the formation of seasonally persistent summertime anoxia in the bottom water under warm summer temperatures (Malone et al. 1986, Kemp et al. 1992, Paerl et al. 1998, Møhlenberg 1999, Rabalais et al. 2007).

Although this mainstem conceptual model of hypoxia formation is appropriate for a number of estuarine systems worldwide, it does not apply as well to conditions that are present within some of the Chesapeake Bay's shallower tributaries. These tributaries are influenced by multiple sources of labile organic matter, advection of high nutrient/low oxygen water from the mainstem, and variable physical mixing processes — both tidally and wind driven (Haas 1977, Kuo & Neilson 1987, Sharples et al. 1994, Fisher et al. 2006, Boynton et al. 2008, Testa & Kemp 2008). Additionally, recent studies have demonstrated the importance of estuarine circulation in advection of nutrients and sometimes hypoxic water from the mainstem into these sub-estuaries (Jordan et al. 1991, Boynton et al. 2008, Testa et al. 2008) as well as in other coastal marine systems (de Jonge 1997, Brush 2004).

The York River estuary (YRE) (Fig. 1) oscillates between stratified and well-mixed conditions due to the physical mixing of the spring-neap tidal cycle (Haas 1977, Hayward et al. 1982, Kuo & Neilson 1987, Diaz et al. 1992). This unique physical mechanism creates the potential for continued formation and disruption of bottom water hypoxia from late May to early September within the lower half of the estuary. Destratification events have the ability to supply regenerated nutrients to the surface water, stimulating phytoplankton production throughout the summer and early fall (D'Elia et al. 1981, Haas et al. 1981).

While previous studies in the YRE have highlighted the interaction between the spring-neap cycle and the occurrence of low oxygen bottom water, we still lack an understanding of how the full suite of biological processes interact with physical stratification in the system (Countway et al. 2007). Until now there has not been an attempt to establish a constrained carbon budget for the York River, which would be achieved by examining the multiple organic matter sources that ultimately drive this system to hypoxia. In addition to internal phytoplankton production, and riverine and offshore inputs of dissolved (DOC) and particulate (POC) organic carbon, contributions to this system from the extensive microphytobenthic community are not well known. An additional driver of hypoxia in the YRE could be advection of water with low dissolved oxygen (DO) concentrations from the lower Chesapeake Bay mainstem as indicated by high-resolution surveys in the lower estuary (Fig. 2a,b). Although the lower mainstem portion of the Chesapeake Bay is not typically considered as a potential source of low DO water, it was classified as an area of low oxygen water in the 1950s (Officer et al. 1984) and more recently identified as an area of hypoxic water separate from the mesohaline mainstem hypoxic/anoxic zone in 1999 (Hagy et al. 2004).

To establish a better understanding of the biological and physical factors controlling organic matter loading and subsequent development of hypoxia in the YRE, a multi-faceted sampling

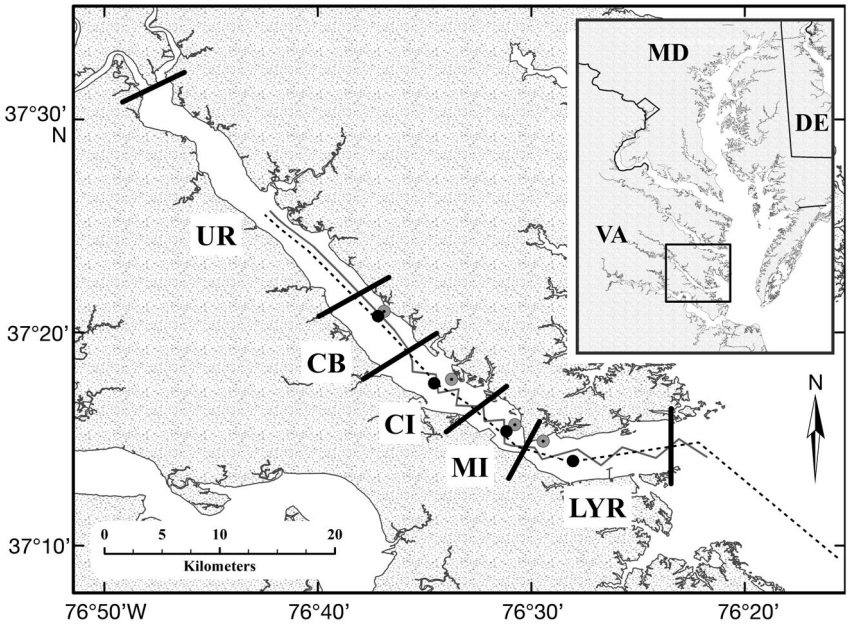

Fig. 1. York River estuary and Chesapeake Bay (inset), including boundaries of each sampling region and corresponding channel (●) and nearshore (◎) sampling stations. Acrobat™ monitoring surveys (grey line) were conducted bimonthly (2007) and monthly (2008) to examine the spatial extent of hypoxia in 3 dimensions. Intensive surveys (dashed black line) were conducted every 2 to 3 d for a 2.5 wk period during June and August of each year to capture the development, spread, and disruption of hypoxia. The intensive surveys were extended outside the mouth of the York River estuary into the lower Chesapeake Bay for the 2008 sampling season. UR: upper river; CB: Clay Bank; CI: Catlett Islands; MI: Mumfort Island; LYR: lower York River

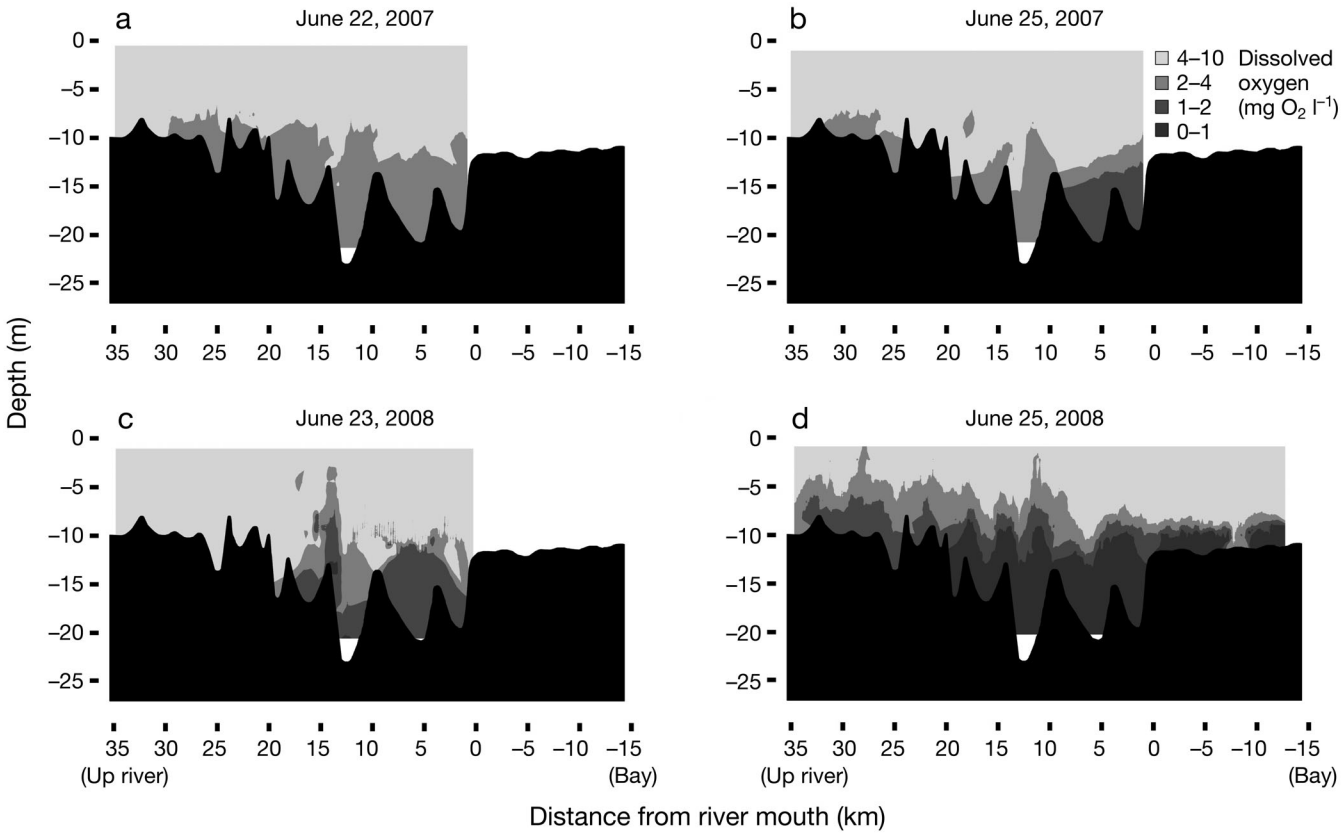

Fig. 2. Interpolated dissolved oxygen concentrations from Acrobat™ surveys. (a,b) June 2007 and (c,d) June 2008. (a,b) Hypoxic water appearing in the lower York River estuary (YRE) following a neap tide on June 22, 2007. (c,d) Water column stratification and hypoxia persisting after a spring tide on June 19, 2008. (d) Hypoxic water was observed in bottom waters up to 13 km outside the mouth of the YRE on June 25, 2008. All Acrobat™ interpolations were developed using the Inverse Distance Weighting method in ArcMAP v. 9.3

program was undertaken during the summers of 2007 and 2008. A series of high-resolution 2- and 3-dimensional surveys of water quality were performed using an Acrobat™ (Sea Sciences) towed undulating platform as part of a larger program to determine the conditions that lead to the formation and disruption of bottom water hypoxia within the estuary. Discrete sampling and metabolic incubations were conducted to assess the effect of the spring-neap cycle on surface water column nutrient concentrations, chlorophyll *a* (chl *a*) concentrations, and surface and bottom water metabolic rates. Measured rates of oxygen consumption were compared to empirical trajectories of oxygen decline over multiple spring to neap tide transitions to assess the potential for internal respiration to account for observed levels of hypoxia in the system, or whether advection of hypoxic water from Chesapeake Bay had to be invoked to fully account for the observed declines. Finally, data were synthesized into a spatially-explicit, temporally-integrated mass balance of carbon to examine the significance of multiple organic matter sources in relationship to hypoxia in the estuary.

MATERIALS AND METHODS

Site description

The YRE is formed by the confluence of the Mattaponi and Pamunkey Rivers near West Point, Virginia, approximately 55 km from where the river enters the mainstem of the Chesapeake Bay on its western edge (Shen & Haas 2004) (Fig. 1). The polyhaline segment of the river extends from the mouth to Catlett Islands (approximately 19 km), and the mesohaline region continues from this point approximately 16 km upstream to the confluence of the Mattaponi and Pamunkey Rivers. Although the surrounding watershed has the second highest population density of the 3 larger Virginia tributaries, the overall land use surrounding the York River proper is

predominantly rural with 62% forested and 16% agricultural land (Dauer et al. 2005).

For this study the YRE was sub-divided into 4 primary sampling regions along its axis (Fig. 1). These regions were designated based on the presence of hypoxia observed during 2007 Acrobat™ monitoring cruises and to cover the portion of the river that has historically experienced hypoxia based on long term water quality monitoring by the EPA Chesapeake Bay Program (CBP). The 2 upstream mesohaline sites located near Clay Bank (CB) and Catlett Islands (CI) were characterized as having little to no signs of hypoxia, while the 2 downstream polyhaline sites Mumfort Island (MI) and the lower York River (LYR) were observed to develop periodic hypoxia during 2007 Acrobat™ monitoring surveys and in previous studies (Kuo & Neilson 1987, Kuo et al. 1993).

Acrobat™ monitoring

As part of a larger water quality monitoring program, the YRE was surveyed during the summers of 2007 and 2008 using an Acrobat™ system equipped with a CTD (Falmouth Scientific Seabird), SCUFA fluorometer/turbidometer (Turner Designs), and a rapid response (300 ms) dissolved oxygen (DO) sensor (AMT Analysenmeßtechnik). Acrobat™ sensors collected spatially-referenced data 4 times a second with a horizontal resolution of 6 to 8 m and a vertical resolution of 5 to 10 cm, for a total of 40000 to 50000 data scans per survey. Prior to deployment and immediately following each cruise, a 2-point calibration was performed on the DO sensor (0 and 100% saturated water). Additionally, DO grab samples were collected at the beginning and end of each cruise and analyzed (standard Winkler titrations) to ensure sensor accuracy (± 0.5 mg l^{-1}).

Monitoring surveys along a zig-zag path were conducted bimonthly (2007) or monthly (2008) to capture the spatial extent of hypoxia in 3 dimensions (Fig.1). A second straight-line, temporally-intensive sampling strategy was used to capture the development, spread, and disruption of individual hypoxic events during June and August of each year. These intensive surveys were conducted every 2 to 3 d for 2.5 wk through a neap-spring-neap tidal cycle, sampling the deepest section of the main channel. For the 2008 sampling season the intensive Acrobat™ cruises were extended approximately 15 km into the lower mainstem of the Chesapeake Bay to identify possible sources of hypoxic water that could be advected into the YRE.

Spring-neap discrete surveys

To collect data on additional water quality parameters and to develop metabolic budgets, a series of 13 water quality surveys and metabolic incubations were conducted from June to September 2008. Sampling dates were selected with a 3 d lag behind the apex of spring and neap tides in order to sample the river at the peak of mixing and stratification, respectively, as indicated by previous studies (Haas 1977, Haas et al. 1981, Hayward et al. 1986) and past Acrobat™ surveys.

At each channel site (Fig. 1) a YSI 6600 series V2 sonde was used to measure temperature, salinity, chlorophyll *a*, and DO at the surface (0.5 m) and at 1 m intervals (starting at 1 m below the surface) to the bottom of the river. All YSI probes were cleaned and calibrated prior to each survey in accordance with YSI's operating manual methods. Conductivity and DO were calibrated using a 0.2 M standard solution of potassium chloride and 100% air saturated water, respectively. Additionally, a 2-point calibration was performed on the optical turbidity and chlorophyll *a* probes using deionized water and YSI conductivity standard or a rhodamine dye standard, respectively. A LiCor LI-1400 was used to measure irradiance through the water column at an intermediate site between the channel and nearshore sites for computation of vertical attenuation coefficients (k_D). Readings were taken just below the surface (<0.1 m) and at 1 m. All YSI and LiCor measurements were obtained in triplicate at each depth.

Surface water samples (0.25 m below surface) were collected at each channel site in 500 ml amber Nalgene bottles and immediately placed on ice until they were transported to the lab. Water column chlorophyll *a* (WC chl *a*) was determined by filtering 15 or 20 ml (depending on concentration) through a Whatman 0.7 µm glass microfiber filter, sealed in aluminum foil, and placed in the freezer. Samples were later removed and extracted in the dark for 24 h in 8 ml of 45:45:10 dimethyl sulfoxide:acetone:reagent water with 1% diethylamine (Shoaf & Lium 1976), and read on a 10 AU Turner Design fluorometer before and after acidification. All WC chl *a* samples were run in triplicate and processed within 1 mo after the initial sampling date. Nutrient samples were filtered through pre-rinsed 0.45 µm Acrodisc filters and frozen until analysis for dissolved inorganic nitrogen (NH_4^+, NO_3^- and NO_2^-), phosphorus (PO_4^{3-}), and silica (Si) on a Technicon AAII Continuous Flow Autoanalyzer.

At each nearshore site (Fig. 1), 3 replicate sediment samples were collected by pole corer for sedi-

ment chlorophyll *a* (SED chl *a*) analysis at a depth of 1 m below mean lower water (MLW), taking into account the daily tidal range. Subsamples of the 0 to 0.3 cm depth fraction of each core were transferred into sterile 15 ml Falcon polypropylene centrifuge tubes (BD Biosciences), and immediately placed in an ice filled cooler and frozen for a maximum hold time of 1 mo. Samples were extracted in 10 ml of a 90% acetone:10% reagent water (by volume) solution, vortexed for 30 s on full power, and sonicated for an additional 30 s at 4 to 5 watts with a Fisher Scientific Dismembranator. After a 24 h extraction period in the freezer, samples were filtered with PALL Life Science HPLC Acrodisc filters (25 mm filter with a 0.45 µm CR-PTFE) and analyzed spectrophotometrically on a Beckman DU 800 Spectrophotometer before and after acidification using the equations of Lorenzen (1967) to correct chl *a* values for phaeophytin.

Metabolic incubations

Surface water, bottom water, and deep channel sediment cores were collected on each survey at each channel site, and shallow water sediment cores were collected monthly at each nearshore site to develop production-irradiance (P-I) curves and compute metabolic rates. Surface water samples were collected in blackened 2 l Nalgene bottles at a depth of approximately 0.5 m. Bottom water samples (1 m above the sediment surface) were collected using a Niskin bottle and immediately transferred into blackened 4 l Nalgene bottles. Deep channel sediment cores (n = 4) were collected during each survey using a box corer, sub-sampled with clear acrylic tubing (height 15 cm: i.d. 4.1 cm) and immediately placed on ice. Nearshore sediment cores (n = 13) were collected at 1 m below mean low water (MLW) in cores of the same size. Sediment height within both the nearshore and deep channel cores was approximately 7 cm, with 8 cm of overlying sample water.

Metabolic rates were determined using the methods of Giordano (2009), Lake & Brush (2011), and Giordano et al. (2012). Water samples were incubated immediately upon returning to the lab. Initial oxygen measurements for metabolic experiments were determined with a HACH HQ 40d oxygen meter with luminescent DO sensors. Ten 60 ml BOD bottles were filled with surface water and incubated at ambient temperatures in temperature-controlled, flow-through light gradient boxes under an increasing gradient of photosynthetically active radiation (PAR, ~50–1600 µE m^{-2} s^{-1}). Four additional surface water samples and 4 bottom water samples were placed in a corresponding temperature-controlled dark box for determination of respiratory rates. Samples were incubated in the light for 1 to 2 h, while dark incubations lasted for 15.5 to 27.5 h, depending on oxygen uptake rates.

Sediment cores were allowed to acclimate uncapped overnight in gently mixed, filtered seawater. Just prior to incubation, the overlying core water was siphoned out of the nearshore cores (taking care to not disturb the sediment surface) and replaced with filtered (0.5 µm) site water with a known DO concentration. Similarly, deep channel cores were siphoned and replaced with unfiltered site water with a known DO concentration. All samples were sealed with polyethylene (Saran Wrap™), which has a low oxygen permeability (5.8×10^{-5} ml cm^{-2} h^{-1}; Pemberton et al. 1996) held in place by a tight rubber band. Once sealed, the cores were placed in light gradient boxes and incubated as described above for approximately 1.5 to 2 h in the light and 2 to 3 h in the dark (n = 10 for nearshore cores in the light; n = 3 for nearshore cores in the dark; and n = 4 for deep channel cores in the dark).

Net community production (light) and respiration (dark) rates for the water and sediments were computed from the change in DO concentrations over the incubation period and normalized to chl *a* biomass (0 to 3 mm for cores). Water column metabolic rates were used to develop a series of production-irradiance (P-I) curves using the equation of Platt et al. (1980) in Statistical Analysis Systems (SAS®), which takes into account photoinhibition:

$$P^B = P^B_s\,[1 - \exp(-\alpha^B I/P^B_s)] \times [\exp(-\beta^B I/P^B_s)] - R^B$$

where net biomass-specific production (P^B, mg O_2 mg chl^{-1} h^{-1}) is dependent on irradiance (I, µE m^{-2} s^{-1}) and 4 statistically determined variables — a term that corresponds to the maximum gross photosynthetic rate in the absence of photoinhibition (P^B_s, mg O_2 mg chl^{-1} h^{-1}), the initial slope of the P-I curve (α^B, mg O_2 mg chl^{-1} h^{-1} (µE m^{-2} s^{-1})$^{-1}$), a negative slope characterizing photoinhibition (β^B, mg O_2 mg chl^{-1} h^{-1} (µE m^{-2} s^{-1})$^{-1}$), and the biomass-specific rate of respiration (R^B, mg O_2 mg chl^{-1} h^{-1}). Sediment incubations were used to develop a similar series of P-I curves using the Jassby & Platt (1976) hyperbolic tangent function:

$$P^B = P^B_{max} \tanh(\alpha^B I/P^B_{max}) - R^B$$

where P^B_{max} is the biomass-specific maximum gross photosynthetic rate (mg O_2 mg chl^{-1} h^{-1}).

Computed oxygen trajectories

To assess the role of internal respiration versus advection of hypoxic water from the Chesapeake mainstem in the formation of hypoxia within the YRE, bottom water and deep channel sediment respiration rates obtained from the metabolic experiments were combined with *in situ* measurements of DO from the Acrobat™ surveys to compare observed and computed declines in bottom water oxygen concentrations in the mesohaline and polyhaline segments during spring to neap tide transitions. Data from 5 Acrobat™ cruises from spring to post neap tidal stage (representing the transition from minimum stratification and highest DO to maximum stratification and lowest DO) during June and August of 2007 and 2008 were used to calculate the volume-weighted change in sub-pycnocline DO concentrations within each segment of the river using the NOAA Chesapeake Bay and Tidal Water Interpolator (http://archive.chesapeakebay.net/cims/interpolator.pdf). Pycnocline depths were set at 5 and 9 m in the mesohaline and polyhaline regions, respectively, based on Acrobat™ results. Sub-pycnocline respiratory oxygen demands were calculated by averaging the rates of bottom water and deep channel sediment respiration from the corresponding sites in the mesohaline (CB & CI) and polyhaline (MI & LYR) segments. These average rates were then linearly interpolated between sampling dates and scaled up by volume (water column) and area (sediment) to obtain segment-wide rates of daily oxygen consumption. Uncertainty around these rates was included by interpolating ±1 standard error in the measured rates between sampling dates. The observed changes in bottom water DO concentrations from the Acrobat™ surveys were then compared to concentrations computed from the interpolated measurements of respiratory oxygen demand with associated uncertainty. Measured metabolic rates from June and August of 2008 were applied to June and August of 2007, respectively, as metabolic incubations were only conducted in 2008. While this calculation assumes that the bottom water was completely isolated from mixing with the surface water and that GPP in this layer was zero, it provides an estimate of what DO trajectories would have been if internal respiration was the sole factor governing oxygen concentrations. These estimates, therefore, provide a first-order constraint in determining whether internal metabolism alone could drive the observed formation of hypoxia below the pycnocline or whether other physical processes, like the advection of low DO water from the mainstem, were required to match the observed DO trajectories.

Carbon budget

P-I parameters were combined with time series of chl *a*, k_D, and incident PAR to generate estimates of daily gross primary production of the water column and benthos (GPP_{WC} and GPP_B, respectively), daily net community production (NCP_{WC} and NCP_B), and daily respiration (R_{WC} and R_B) for each region of the YRE. First, estimated values for P^B_{max}, P^B_s, α^B, β^B, R^B, and k_D for each station and cruise were linearly interpolated between sampling dates. Second, YSI depth profiles of WC chl *a* were binned in 0.5 m intervals from the surface to 5 m, since measured attenuation coefficients indicated that photic depths (1% of surface irradiance) were less than 5 m at all sites throughout the sampling period. YSI chl *a* readings were scaled to extracted chl *a* by normalizing the YSI values at depth to the surface reading (0.5 m) and multiplying all values by the extracted surface concentration. SED chl *a* biomass was also binned in 0.5 m intervals by applying a biomass-depth curve developed from extracted samples as part of a larger microphytobenthic (MPB) biomass study along the entire estuary (authors' unpubl. data). This biomass-depth curve was developed from 3 sampling events at 6 stations in the estuary during the spring, summer, and fall of 2009. SED chl *a* was measured at 0.25 m below mean low water (MLW), and in 0.5 m intervals from the surface to 2.5 m below MLW. Biomass-depth curves were expressed as a fraction of the maximum SED chl *a* along each depth transect (values deeper than 2.5 m were calculated based on linear extrapolation of biomass using the rate of change between 2 and 2.5 m MLW); seasonal biomass-depth curves were combined with measured SED chl *a* concentrations from 2008 at 1 m MLW to reconstruct SED chl *a* on each sampling date from 0 to 4 m in 0.5 m bins. All water column and sediment chl *a* values were then interpolated in each depth bin between sampling dates to generate daily values over the study.

Third, PAR data from the Chesapeake Bay National Estuarine Research Reserve meteorological station at Taskinas Creek, Virginia (May to November 2008) were downloaded (www.nerrs.noaa.gov) and used to calculate average hourly instantaneous PAR ($\mu E\ m^{-2}\ s^{-1}$) for the study period. Finally, bathymetric soundings were downloaded from the NOAA

National Geophysical Data Center (www.ngdc.noaa.gov) and interpolated using a kriging function in ESRI ArcMAP GIS v. 9.3, to a 5 m × 5 m grid with a resolution of 10 cm in the vertical. The surface area and volume within each sampling region (Fig. 1) was computed in 0.5 m depth intervals from mean sea level (MSL) to the bottom.

Interpolated time series of P-I parameters, k_D, chl *a* biomass, and hourly PAR were used to compute hourly gross primary production and respiration of water and sediments over 0.5 m depth intervals in each region of the YRE. Metabolic rates from CB were applied to the adjacent upper river (UR) region, from CB up to the head of the estuary (Fig. 1). Constant photosynthetic and respiratory quotients of one were applied to all sites to convert from oxygen to carbon units (Kemp et al. 1997, Smith & Kemp 2003). While photosynthetic and respiratory quotients are variable (Laws 1991, Harding et al. 2002), a direct comparison has not been made for the YRE. Hourly metabolic rates were integrated over depth and time to produce site-specific daily values; these rates were then integrated over area, volume, and time to obtain monthly and seasonal region- and estuary-wide estimates of GPP and net ecosystem metabolism (NEM) (GPP minus R). Integrated sediment respiration was computed by area-weighting shallow and deep rates by the sediment surface area above and below the pycnocline, calculated using the NOAA bathymetric data.

To compare these internal carbon sources to external inputs, dissolved organic carbon (DOC) and particulate organic carbon (POC) concentrations at the head (CBP site RET 4.3) and mouth (CBP site WE4.2) of the YRE (Fig. 1) were downloaded from the CBP website (www.chesapeakebay.net). Bottom water DOC concentrations at site WE4.2 were unavailable; values were estimated by multiplying the surface water DOC to POC ratio by the bottom water POC concentration on each sampling date. Daily river flows for the Mattaponi and Pamunkey Rivers were downloaded from the Virginia USGS website (http://va.water.usgs.gov) and scaled to the entire YRE watershed including the area below the fall line. An Officer (1980) box model was used to calculate the exchange rates between the LYR and the Chesapeake Bay using interpolated CBP salinity values measured throughout the system. These freshwater flows and computed exchanges with the Chesapeake were combined with daily interpolated DOC and POC concentrations to estimate input and export of organic carbon across the upstream and downstream boundaries.

Estimating and scaling uncertainty

The inclusion of error estimates in budget calculations of this kind are necessary in order to identify the relative uncertainty associated with each term, and are also useful in determining what input terms need to be focused on in future studies. The magnitude of uncertainty related to various input terms (e.g. chl *a*, k_D, P-I parameters, respiration rates) used to construct this carbon budget have been included on figures as standard error. These calculations follow the framework laid out in Boynton et al. (2008) and Lehrter & Cebrian (2010). The uncertainty associated with computing daily primary production from input terms with associated standard errors was calculated by performing a series of Monte Carlo simulations where chl *a*, k_D, and all associated P-I parameters were randomly selected from their normal distributions. A series of 1000 independent simulations were conducted for both water column and sediment production rates for each site on each sampling date. GPP rates are presented as the mean of those 1000 simulations ±1 standard deviation. Initial testing with the Monte Carlo approach indicated that 500 simulations were sufficient to constrain the standard deviation. This exercise provides estimates of the uncertainty around our measured daily rates, but we have not attempted to propagate error in our daily interpolations between sampling dates or into our seasonal mass balance of organic carbon as that is beyond the scope of the present study.

RESULTS

Water column variability and the spring-neap cycle

During the first half of the summer, the York River experienced 2 periods of strong density stratification (bottom to surface, Δ sigma-t > 2 kg m^{-3}) that were prevalent over consecutive sampling periods (Fig. 3c). These prolonged events were longer in duration and did not follow the typical spring-neap tidal cycle. The first prolonged event during June resulted from storms that initially disrupted stratification during a neap tide, but which was subsequently followed by a significant pulse of fresh water that acted to stratify the system for a 2 wk period (Fig. 3a,c). During mid-July, a relatively weak spring tide did not lead to the complete breakdown of stratification in the 2 polyhaline sampling sites (Fig. 3b,c). Finally, during mid-August, stratification completely broke down throughout the entire river due to a

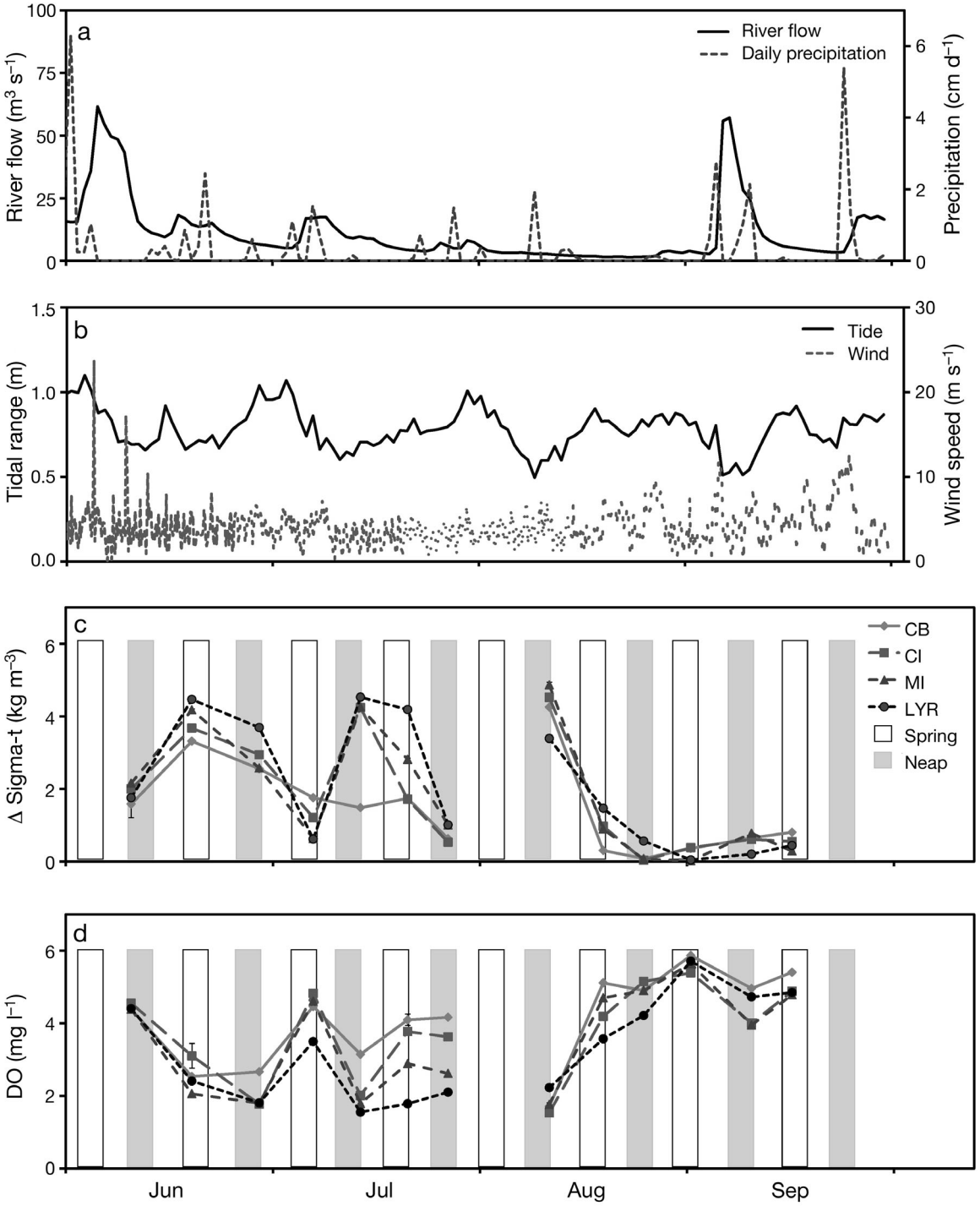

Fig. 3. Time-series of environmental conditions during the weekly spring-neap surveys in 2008. (a) Precipitation at the Taskinas Creek, Virginia meteorological station (www.nerrs.noaa.gov) and combined river flow of the Mattaponi and Pamunkey Rivers (waterdata.usgs.gov/nwis), (b) hourly wind speed and daily tidal range measured at the Coast Guard Pier in the lower YRE (tidesandcurrents.noaa.gov), (c) observed strength of stratification (bottom–surface, sigma-t), and (d) observed mean bottom water dissolved oxygen concentrations. The YRE oscillated between stratified (low oxygen) and well mixed (normoxic) conditions on time scales longer than the spring-neap tidal cycle. Error bars on panels (c) and (d) are standard error. White boxes (outlined in black) highlight a 3 d period beginning at the apex of spring tide; light grey boxes correspond to a 3 d period beginning at neap tides. CB: Clay Bank; CI: Catlett Islands; MI: Mumfort Island; LYR: lower York River

series of strong storm events that acted to completely mix the water column (Fig. 3a-c). Although the lower estuary did not experience stratification during each neap tide, hypoxia did develop during each strong stratification event (Fig. 3c,d). Surface nutrient concentrations did not show an apparent pattern related to the spring-neap cycle (Fig. 4a-c). DIN concentrations remained low throughout June and July until the middle of August, at which point the water column stratification began to break down. DIP concen-

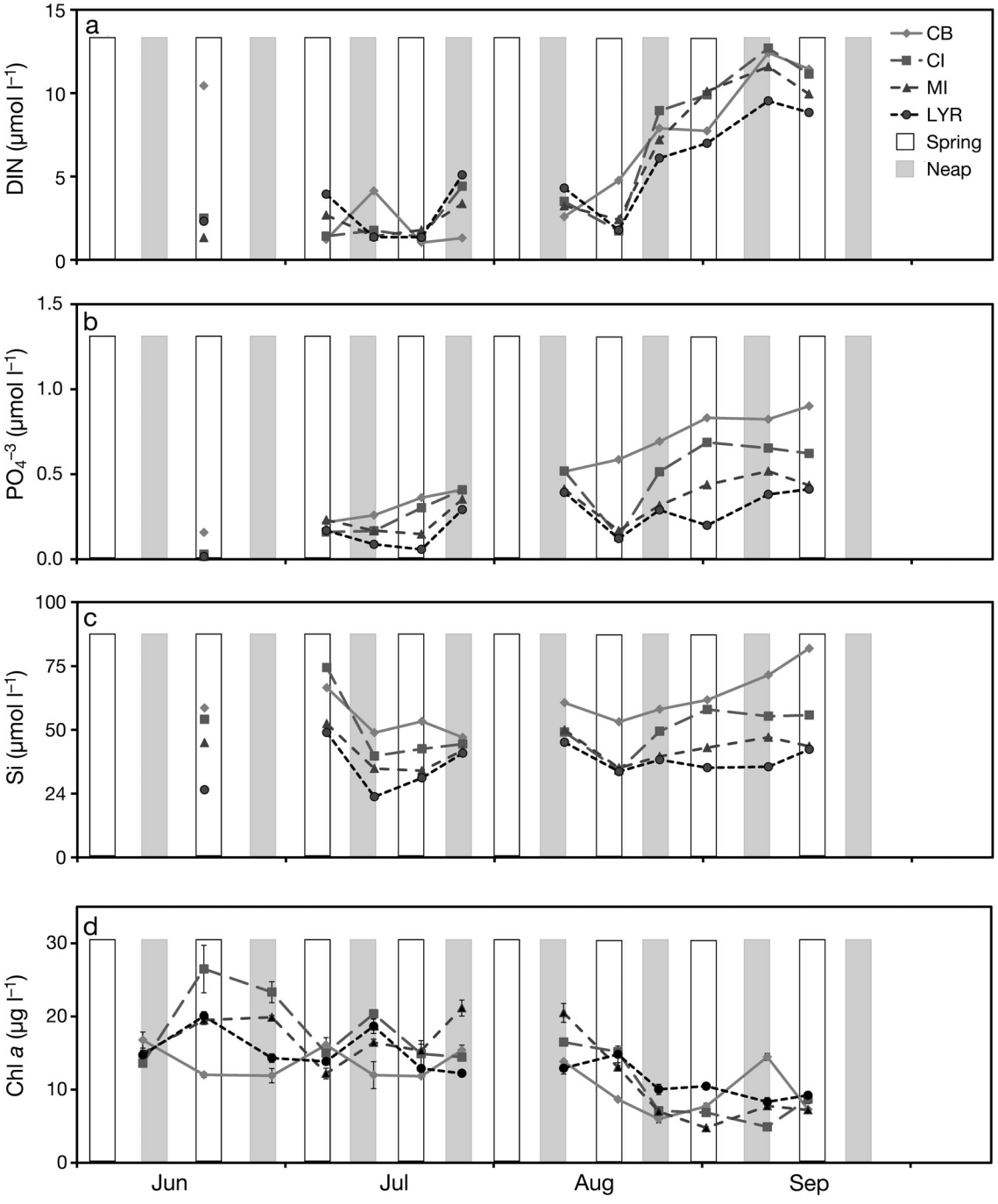

Fig. 4. Nutrient and water column chl *a* concentrations from spring-neap surveys sampled weekly in each sampling region during 2008. (a) Dissolved inorganic nitrogen, (b) dissolved inorganic phosphorus, (c) dissolved silica, and (d) chl *a* concentrations in the surface water (sampled at 0.25 m). Error bars represent standard error. White boxes (outlined in black) highlight a 3 d period beginning at the apex of spring tide; light grey boxes correspond to a 3 d period beginning at neap tides. See Fig. 3 for details of sampling region abbreviations

trations were also low in early June, increasing slightly at some locations during the summer before a brief period of decline in mid-August. DIP at all locations increased in late August and throughout September. Silica concentrations remained elevated, compared to DIN and DIP, from June to September 2008. In contrast to nutrients, surface chl *a* concentrations displayed oscillations in early summer in part related to the spring-neap cycle, with a tendency for higher concentrations during more stratified neap tides (Fig. 4d). Chl *a* concentrations decreased in late August following late summer storm events (Fig. 3b). Measured k_D was lower throughout the sampling period in the LYR (mean value 1.17 m^{-1}) compared to the other regions in YRE (CB 1.79, CI 1.77, and MI 1.43 m^{-1}). However, photic depth (1% of surface irradiance) never exceeded 5 m in any region on any sampling date.

Metabolic incubations

Water column maximum photosynthetic rates and integrated daily production (GPP_{WC}) varied throughout June, July and August with no clear relationship to the spring-neap tidal cycle (Figs. 5a & 6a). Sediment maximum photosynthetic rates and integrated daily production (GPP_B) remained constant at most sites from June to July before decreasing in August and September (Figs. 5b & 6b). Throughout the study, the maximum sediment photosynthetic rates in the LYR remained elevated compared to other 3 regions of the YRE (Fig. 5b). Surface and bottom water column respiration rates exhibited seasonal and shorter-term peaks with the highest rates occurring during mid-summer (Fig. 5c,d). Similarly, shallow sediment respiration rates peaked in mid-summer, while deep channel rates increased initially

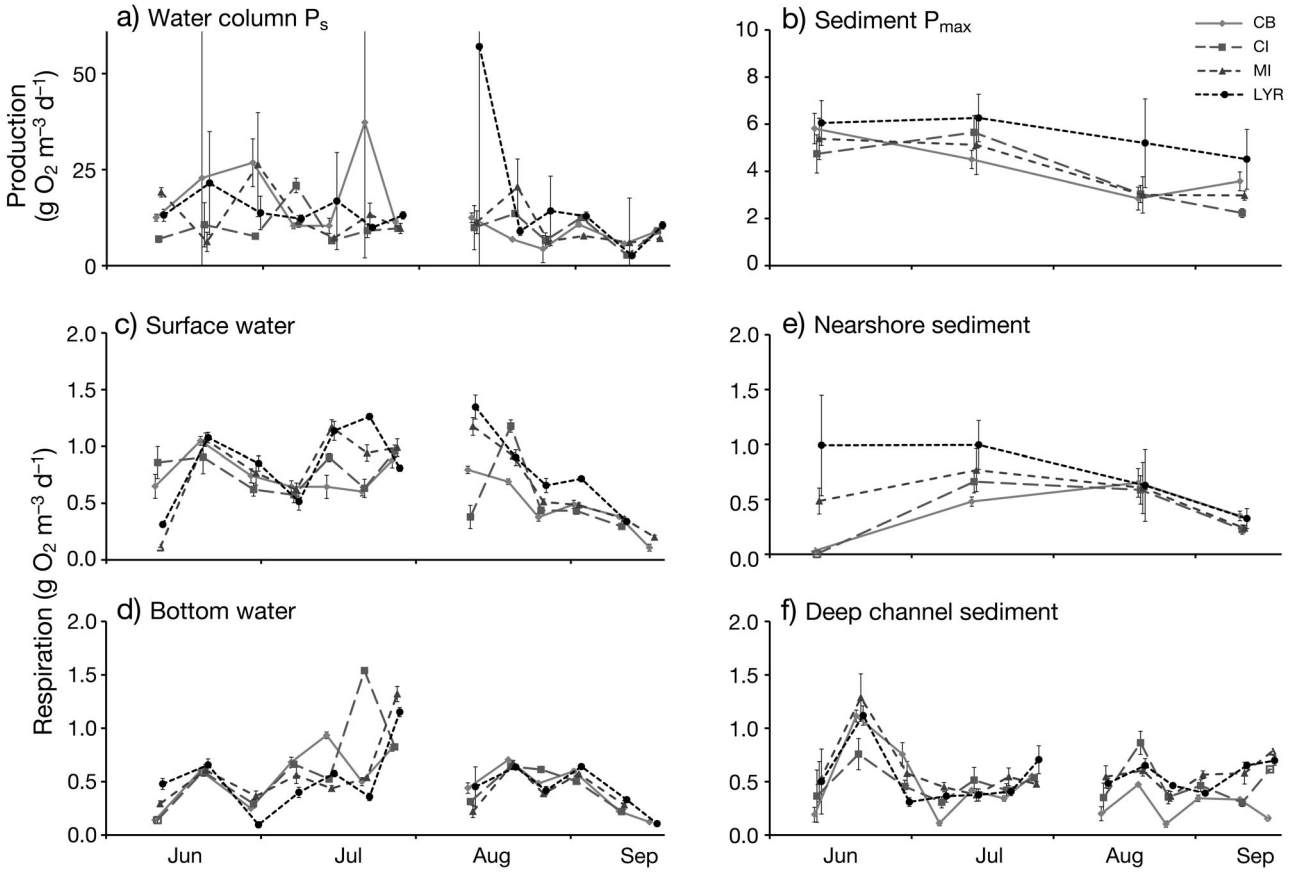

Fig. 5. Time-series of (a) water column and (b) sediment maximum gross photosynthetic rate (in the absence of photoinhibition) measured during light box metabolic incubations following the spring-neap surveys. Hourly biomass-specific values were multiplied by chl *a* biomass and scaled to daily rates to 24 h of continuous irradiance. Lower panels show mean respiration rates for (c) surface (0.5 m) and (d) bottom water, and (e) shallow and (f) deep channel sediments. Hourly biomass-specific values were multiplied by chl *a* biomass and scaled to daily rates. Error bars on all panels represent standard error. Open symbols correspond to dates when fewer than 3 replicates were available or error estimation was not possible due to lack of required data. Mean rates are offset in time to limit overlap of means and error bars. See Fig. 3 for details of sampling region abbreviations

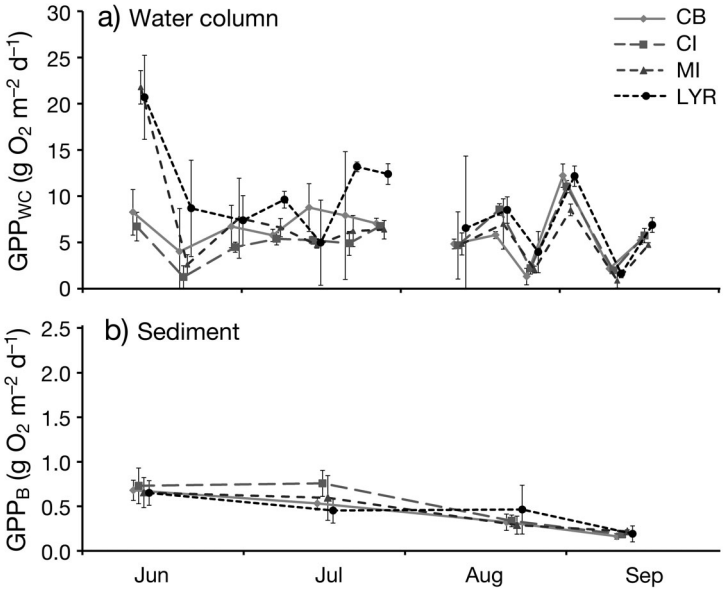

Fig. 6. Mean (a) water column and (b) sediment gross primary production (GPP_{WC} and GPP_B, respectively) calculated from 1000 Monte Carlo simulations where chlorophyll *a*, k_D, and P-I parameters were randomly selected from their normal distributions. Error bars represent the standard deviation of all 1000 simulations. Mean rates are offset in time to limit overlap of means and error bars. See Fig. 3 for details of sampling region abbreviations

in mid-June before decreasing at all sites from July to early August (Fig. 5e,f). During mid-August deep channel respiration rates increased slightly as a series of storms broke down stratification throughout the river (Fig. 3a–c).

Computed oxygen trajectories: advection versus internal consumption

Volume-weighted, sub-pycnocline DO concentrations during the 2007 intensive Acrobat™ surveys covering 2 spring-to-neap transitions declined by an average rate of 0.17 and 0.29 mg O_2 l^{-1} d^{-1} in the mesohaline, and 0.29 and 0.28 mg O_2 l^{-1} d^{-1} in the polyhaline region of the lower YRE during June and August, respectively (Fig. 7a,b). During the intensive surveys in June 2008, DO concentrations initially increased due to a spring tide mixing event (Fig. 3b,c), after which they declined at a rate of 3.43 and 0.15 mg O_2 l^{-1} d^{-1} in the mesohaline and polyhaline zones, respectively (Fig. 7c). During August 2008, DO concentrations in the mesohaline and polyhaline continually increased following a neap tide, which corresponded with the breakdown of stratification within both regions (Figs. 3c & 7d). DO trajectories computed using measured rates of respiration in bottom water and deep channel sediments in 2008 matched or fell below the computed decrease in volume-weighted DO based on Acrobat™ data — except in the mesohaline region during June 2008 (Fig. 7a–d). These trajectories were computed starting at the

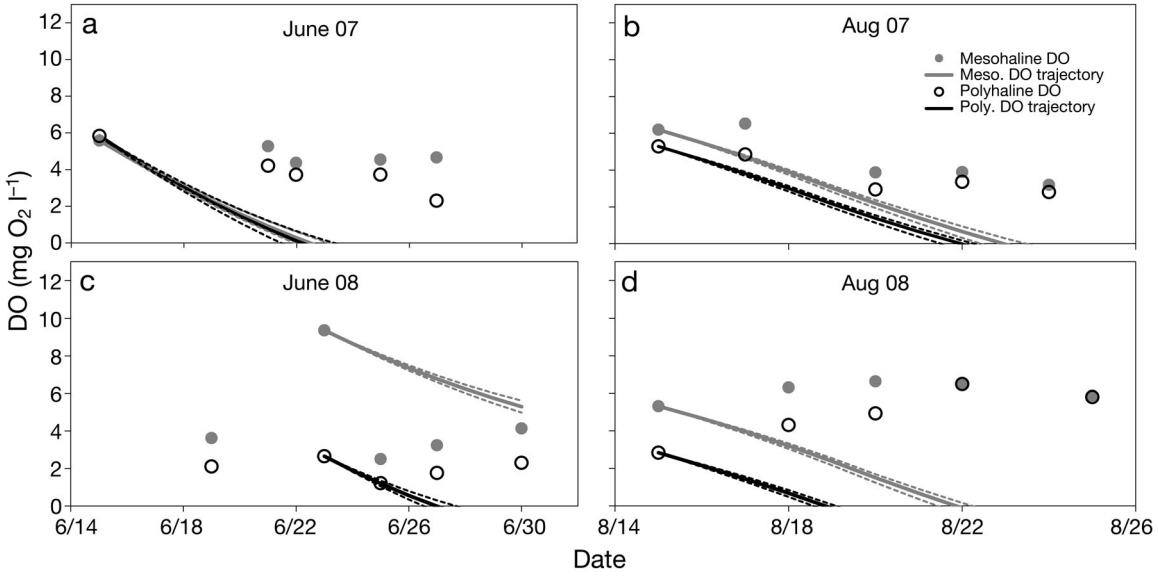

Fig. 7. Computed and observed dissolved oxygen trajectories during spring to post-neap tide transitions. Points represent sub-pycnocline, volume-weighted concentrations in the mesohaline (●) and polyhaline (○) regions of the YRE from Acrobat™ surveys. Lines represent the expected dissolved oxygen trajectories based on measured rates of bottom water column and deep channel sediment respiration for the mesohaline (solid grey) and polyhaline (solid black) regions of the estuary. Dashed lines give the uncertainty in the computed trajectories by propagating ±1 standard error in the measured rates of respiration

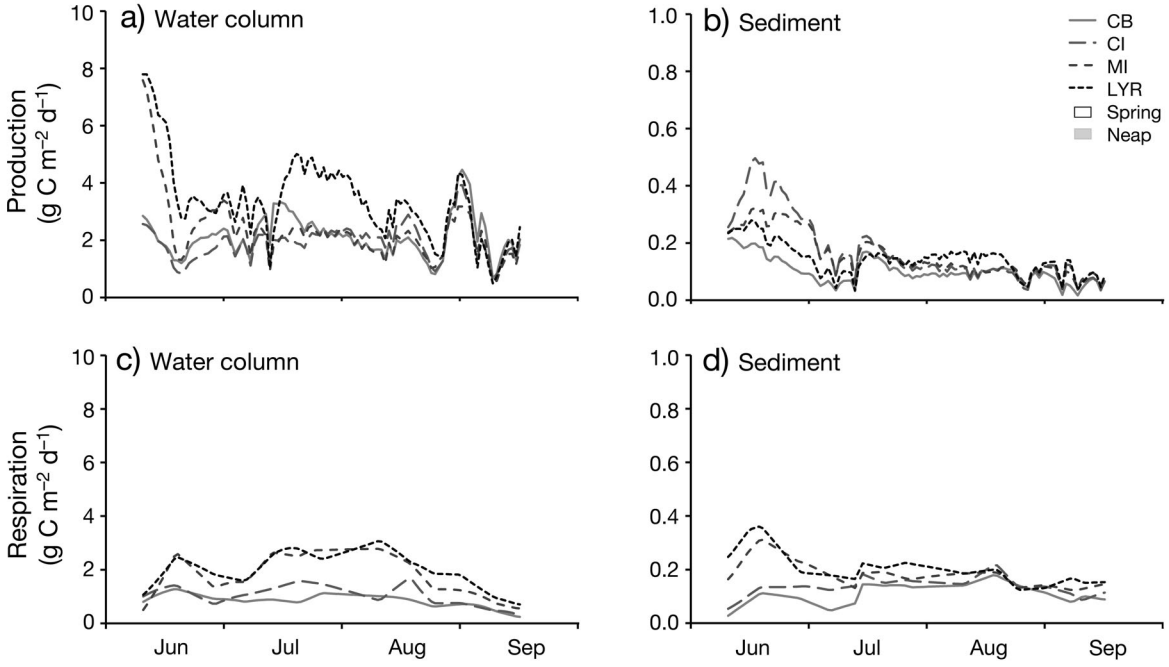

Fig. 8. Interpolated daily (a) water column and (b) sediment gross primary production, and (c) water column and (d) sediment respiration for each sampling region. Values are scaled to each region using hourly PAR and interpolated k_D, chlorophyll *a* in 0.5 m depth bins, and P-I parameters

initial observed concentration except in June 2008, where a mixing event occurred following this initial survey that increased bottom water DO concentrations; in that case, the trajectories were computed from the second observation, after which hypoxia developed. These trajectories provide a first-order estimate of what oxygen concentrations would have been if they were controlled solely by internal respiration, and suggest that in most cases internal respiration was more than sufficient to cause the observed patterns in bottom water DO. The exception was in the mesohaline zone in June 2008, where respiration could not account for the observed rapid decline in DO concentrations; in this case, other mechanisms such as advection of hypoxic water from the polyhaline zone of the estuary must be invoked.

Carbon budget: internal versus external sources

Daily interpolated rates of GPP_{WC} for the YRE oscillated on weekly as well as longer time scales throughout the summer of 2008 (Fig. 8a). However, the realized effect of the spring-neap tidal cycle was overshadowed by longer temporal shifts in WC chl *a* biomass (Fig. 4d) and greater light availability in the LYR during mid summer (which exceeded all other regions during this period). Additionally, interpolated GPP_{WC} initially increased at all sites in late August as stratification broke down before subsequently decreasing for the remainder of the study (Fig. 8a). Although rates varied throughout the summer, mean monthly total gross primary production (GPP_{total}, water column and benthic) generally decreased over the course of the summer (Table 1), with less than 10% of total system gross primary production attributed to the MPB (Fig. 8a,b).

Daily interpolated rates of R_{WC} in the YRE did not appear to respond to the spring-neap cycle (Fig. 8c). Mean R_{WC} increased from June (1.12 g C m^{-2} d^{-1}) to July and August (1.35 g C m^{-2} d^{-1}), before declining to the lowest seasonal rates in September (0.55 g C m^{-2} d^{-1}) (Table 1, Fig. 8c). Rates at Stations CB and CI remained relatively constant throughout the summer with short periods of higher values, while rates at MI and LYR increased in mid June to approximately double the rates of CB and CI and remained elevated until late August. Daily interpolated rates of benthic respiration (shallow and deep sediments combined) increased slightly from June to August (0.16 g C m^{-2} d^{-1}) with an average seasonal rate of 0.14 g C m^{-2} d^{-1}), which accounted for approximately 11% of total system respiration throughout the summer (Table 1, Fig. 8c,d).

Table 1. Monthly and seasonal mean rates of integrated gross primary production (GPP), respiration (R), and net ecosystem metabolism NEM (GPP_{total} – R_{total}) for the entire York River estuary. Total GPP and R are the sum of water column (WC) and benthic (B) rates. Values may not sum due to rounding. Seasonal totals are integrated across daily interpolated rates and are not an average of the monthly values

	York River estuary metabolic rates (g C m^2 d^{-1})				
	Jun	Jul	Aug	Sep	Seasonal mean
GPP_{total}	2.97	2.31	1.87	1.73	2.22
GPP_{WC}	2.78	2.21	1.78	1.67	2.11
GPP_B	0.20	0.10	0.09	0.05	0.11
R_{total}	1.25	1.49	1.51	0.66	1.23
R_{WC}	1.12	1.35	1.35	0.55	1.09
R_B	0.13	0.14	0.16	0.11	0.14
NEM	1.72	0.82	0.36	1.07	0.99

Table 2. Monthly and seasonal mean net ecosystem metabolism (NEM = GPP_{total} – R_{total}) for each region of the York River estuary. Seasonal totals are integrated across daily interpolated rates and are not an average of the monthly values. See Fig. 1 for details of sampling region abbreviations

Region	Net ecosystem metabolism (g C m^2 d^{-1})				
	Jun	Jul	Aug	Sep	Seasonal mean
UR	0.70	0.53	0.06	0.74	0.50
CB	1.21	1.40	0.76	1.55	1.23
CI	0.77	0.54	0.86	1.34	0.88
MI	3.37	–0.12	–0.53	0.79	0.86
LYR	3.74	1.22	0.30	0.96	1.54

Regional rates of NEM varied temporally and spatially throughout the river, with the highest rates of net autotrophy occurring during June in MI and LYR, and during September in CB and CI (Table 2). Most regions remained net autotrophic throughout the entire summer, although NEM at UR and LYR decreased to 0.06 and 0.30 g C m^{-2} d^{-1}. However, at MI, NEM decreased from 3.37 g C m^{-2} d^{-1} in June to –0.12 g C m^{-2} d^{-1} in July and remained net heterotrophic through August (–0.53 g C m^{-2} d^{-1}). Seasonal NEM for the whole system decreased from June to August with a rebound in September as water column production increased and respiration rates declined (Table 1).

Since the rates of internal oxygen consumption appeared sufficient to drive development of bottom water hypoxia in the lower YRE, results from the metabolic incubations were used to construct a carbon budget for the system to identify the potential roles of autochthonous and allochthonous carbon sources in driving hypoxia. In addition to phytoplankton and MPB production, this analysis incorporated external sources of organic carbon from tributaries, the surrounding watershed, and Chesapeake Bay. Results indicated that the monthly average net input of DOC and POC from the 2 tributaries ranged from 5.5 × 10^3 to 2.2 × 10^4 kg C d^{-1} during the summer, with an average seasonal rate of 1.2 × 10^4 kg C d^{-1}. The smaller watersheds that surround the YRE supplied an average of 866 kg C d^{-1} (monthly means ranging from 200 to 6800 kg C d^{-1}). However, both of these sources were relatively low compared to the seasonal mean import (2 × 10^5 kg C d^{-1}) and export (2.1 × 10^5 kg C d^{-1}) of organic carbon from the Chesapeake Bay.

DISCUSSION

Drivers of water column dynamics

The 2008 Acrobat™ and spring-neap surveys confirmed the importance of density stratification and the development of hypoxia within the YRE; however, the spring-neap tidal cycle did not completely drive the oscillations between stratified and non-stratified periods (Fig. 3c). A series of strong storms during early June acted to break down stratification over a neap tidal period, while the subsequent freshwater input following the storms stratified the system during a relatively weak semidiurnal spring tide (Fig. 3a–c). During mid-July, stratification in the polyhaline York River did not fully break down until more than 3 d after a weaker spring tide. However, the system remained homogenous through the following neap tide due to stronger than predicted neap tidal amplitudes. Finally, during mid-August, stratification completely broke down throughout the entire river due to a series of strong storm events that acted to completely mix the water column (Fig. 3a–c). High resolution sampling confirmed that the spring-neap cycle has the ability to control stratification and hypoxia, as noted in other previous studies (Haas 1977, Hayward et al. 1982, Kuo & Neilson 1987). However, the results also indicated a number of other important physical factors that must also be considered, e.g. strong wind events, freshwater flow, and relative tidal mixing strength.

Metabolic rate measurements

The metabolic rates observed in this study were within the range or slightly below those reported from previous studies conducted in the lower polyhaline Chesapeake Bay. Kemp et al. (1997) reported seasonal GPP rates for June to September between 0.75 and 5.25 g C m^{-2} d^{-1} in the lower bay (assuming a PQ = 1). Seasonal mean GPP_{WC} values in this study fell within their range, at 2.11 g C m^{-2} d^{-1} (monthly means from 1.73–2.97 g C m^{-2} d^{-1}), with maximum daily values exceeding 4 g C m^{-2} d^{-1} (Fig. 8a). The net water column primary production rates in this study ranged from 0.43 to 1.66 g C m^{-2} d^{-1}, which spanned the summer net ^{14}C primary production value of 1.2 g C m^{-2} d^{-1} reported by Harding et al. (2002) for the lower bay. However, these net rates fell below the daytime net community production values reported by Smith & Kemp (1995) (3.53 ± 0.83 g C m^{-2} d^{-1}). R_{WC} rates from this study (0.012–0.056 mg O_2 l^{-1} h^{-1}) overlapped the mean values reported for the lower bay above 20°C by Smith & Kemp (1995) for the surface layer (0.01–0.04 mg O_2 l^{-1} h^{-1}). Similarly, R_{WC} for the bottom layer (0.001–0.055 mg O_2 l^{-1} h^{-1}) of the YRE also overlapped Smith & Kemp (1995) lower bay rates (0.01–0.04 mg O_2 l^{-1} h^{-1}). The measured deep channel sediment oxygen demand rates spanned the range reported for the lower Chesapeake Bay during summer and early fall (0.65–0.75 g O_2 m^{-2} d^{-1}) by Cowan & Boynton (1996) (Fig. 5f). However, the scaled YRE monthly average rates were slightly below this range (0.42–0.66 g O_2 m^{-2} d^{-1}).

Computed oxygen trajectories

Comparing *in situ* DO concentrations over the intensive Acrobat™ surveys in 2007 and 2008 with trajectories computed using rates from the 2008 metabolic incubations (Fig. 7) provides an estimate of the role of respiration in controlling the observed changes in DO concentrations. While this exercise is admittedly first-order as it excludes mixing of oxygen across the pycnocline and assumes that the rates during 2007 were the same as 2008, it nevertheless provides a method for quantifying the relative importance of internal respiration as opposed to external factors (like advection of hypoxic water into the system from the lower Chesapeake Bay). The other major process that was excluded from these calculations is production of oxygen below the pycnocline. However, calculations based on measured attenuation of irradiance and P-I curves indicated minimal to no photosynthetic oxygen production below approximately 5 m, the depth used for the mesohaline pycnocline in these calculations (9 m in the polyhaline).

The comparison of *in situ* and computed DO concentrations within the polyhaline YRE indicated that internal respiration alone was capable of driving this system to hypoxia under stratified conditions without the need for advection of hypoxic water from the Chesapeake Bay (Fig. 7). During the summer of 2007, the interpolated volumetric DO concentrations in the polyhaline declined at rates less than or equal to the combined water column and sediment respiration trajectories. During June of 2008, the DO concentrations in the polyhaline YRE initially declined slightly faster than suggested by respiratory rates; however, this may be due in part to a settling effect of higher density low DO water that was partially mixed into the surface layer during the previous spring tide (Fig. 2c,d). The 2007 mesohaline oxygen concentrations also declined at rates equal to or less than the oxygen uptake trajectories measured for this region. During June of 2008, however, the observed DO concentrations for the mesohaline YRE declined much faster than those computed from metabolic rates, which suggests that factors other than internal respiration were required to explain the observed decline. In this instance, it appears that the rapid decline in DO concentrations was caused by the advection of low DO water into the mesohaline region from the polyhaline YRE. Acrobat™ surveys from 2008 appear to confirm this, as higher density low DO water advanced upriver following a spring tide (data not shown). DO concentrations in both the polyhaline and mesohaline increased throughout the month of August (2008), as fall storms mixed the entire water column for the remainder of the summer (Fig. 3a,b).

Summer integrated GPP and R

Confirmation that internal respiration within the estuary was generally sufficient to drive hypoxia led to an evaluation of the importance of individual autochthonous and allochthonous organic matter sources and their potential to contribute to hypoxia at monthly and seasonal scales. While uncertainty was not propagated through the daily interpolated estimates of GPP and R (Fig. 8) used to generate the values in Table 1, the estimated error associated with

the measured rates (Figs. 5c–f & Fig. 6) indicates that the values are sufficiently well constrained to allow order of magnitude comparisons between water column and sediment rates, contributions from phytoplankton and MPB, and relative rates of production and respiration. Results indicated that phytoplankton production dominated total GPP in the system and was more than sufficient to offset the aerobic respiration in the water column and sediments (Table 1). This study did not capture the spring phytoplankton bloom in the tributaries and upper river that precedes seasonal development of hypoxia in the polyhaline segment, which would provide an additional phytoplankton-based source of carbon for fueling hypoxia.

Microphytobenthic production has been suggested to be an important source of autochthonous carbon throughout the year in the York River (Buzzelli 1998) and similar shallow systems (Pinckney & Zingmark 1993, Reay et al. 1995). These results indicate that benthic production accounted for less than 10% of GPP_{total} throughout the summer, which is similar to the microphytobenthic production contribution for the mainstem Chesapeake Bay estimated by Kemp et al. (1999). However, on a local scale, benthic production appeared to be more significant in some regions — specifically CI — where GPP_B accounted for up to 20% of GPP_{total} during the month of June before declining to less than 10% in July. Measured benthic production rates were consistently higher in the LYR throughout the summer compared to the other regions (Fig. 5b); however, the high rates of primary production did not offset the smaller percentage of photic surface area in the polyhaline zone (Fig. 8b).

Water column respiration in the mesohaline remained relatively constant from June to late August 2008 with only short weekly periods of elevated rates, which may be due in part to resuspension of the bottom boundary layer resulting from stronger tidal currents. Bed erodibility in this region, which has been demonstrated to be higher than in the lower polyhaline (Cartwright et al. 2009), likely suspends some labile particular organic matter and pore water nutrients into the overlying water column, increasing water column respiration rates. Within the polyhaline regions, R_{WC} rates increased in mid-July, as GPP_{WC} decreased, and remained elevated compared to the mesohaline regions throughout the summer (Fig. 8c). Elevated polyhaline R_{WC} rates were approximately double the corresponding rates in the mesohaline during July and August, which likely resulted from the degradation of internally produced organic matter resulting from greater light availability in the LYR, and advected labile DOC and POC water from the lower Chesapeake Bay.

Spatial and temporal variations in NEM

NEM varied both temporally and spatially throughout the river during the summer of 2008. During June, all sites were found to be net autotrophic with the highest rates of GPP_{total} occurring in MI and LYR (Table 2). With the exception of MI, all regions remained net autotrophic throughout the summer, although the UR and LYR regions decreased to their lowest rates in August. However, MI alternated from net autotrophy to net heterotrophy in July, and remained net heterotrophic through August. Mumfort Island, which is just below the mesohaline–polyhaline transition zone, appears to be a trap for respirable organic matter. This region is also the most upriver location for recurring hypoxia based on previous Acrobat™ surveys (authors' unpubl. data). The CI region, just above MI, is a transition zone where the York River channel becomes wider and deeper compared to the broad shallow regions in the upper river. It is possible that estuarine circulation transports and retains labile organic matter in this region, which results in higher respiration rates within the water column and in the sediments (Fig. 8c,d) without the elevated rates of GPP_{WC} present in the LYR (Fig. 8a).

Seasonal mean NEM for the entire system decreased from June to August with a subsequent increase in September as water column production increased and respiration declined. Interestingly, Raymond et al. (2000) calculated that the York River, including portions of the tributaries, was net heterotrophic using open water DIC measurements. Raymond et al. (2000) also noted that the LYR region had the lowest rates of heterotrophy with seasonal net autotrophy. The discrepancy between Raymond et al. (2000) and this study may be due in part to the 2 different approaches used to measure NEM (*in situ* measurements of DIC versus component incubations). Although there have only been a limited number of studies that have utilized multiple NEM methods, these studies have highlighted discrepancies in NEM values associated with different techniques (Kemp & Boynton 1980, Kemp et al. 1997, Giordano et al. 2012). It is also likely that the DIC method of Raymond et al. (2000) accounted for excess CO_2 from upriver tidal freshwater marsh systems, rather than water column processes within the estuary (Neubauer & Anderson 2003).

Summer total organic carbon budget

Measured biological rate processes and computed physical transport of particulate and dissolved organic carbon from the surrounding watershed and lower Chesapeake Bay were combined into a seasonal budget of organic carbon fluxes in the YRE (Fig. 9). As noted above, estimated errors on the rates each day of measurement (Figs. 5c–f & Fig. 6) are sufficiently well constrained to allow order of magnitude comparisons between major terms in the carbon budget even though errors were not propagated through these seasonal integrated values.

During the summer of 2008, internal water column production accounted for over half (57.5%) of all organic carbon inputs to the YRE, with advected POC and DOC from the lower Chesapeake Bay accounting for an additional 37%. It is not surprising that these 2 sources of organic carbon contributed significantly to this system; past studies of particulate and dissolved organic matter in the YRE have highlighted their significance within the mesohaline and polyhaline portions of the river (Countway et al. 2007, McCallister et al. 2006a,b). Previous studies also indicate that organic matter from the Chesapeake Bay is important to bacterial secondary production within the LYR, contributing 66 to 70% of bacterial production during October (McCallister et al. 2004); however, the contribution during the summer was reported to be significantly lower (8 to 10% in July).

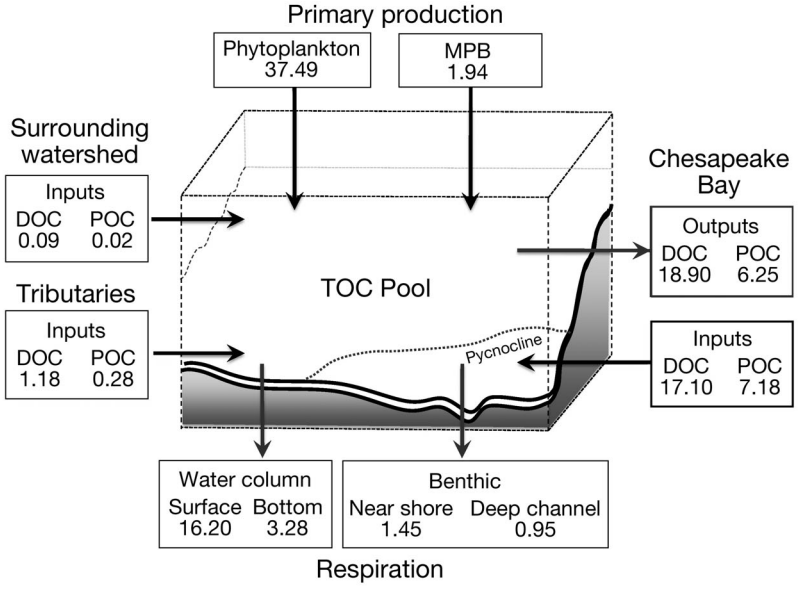

Fig. 9. Estimated total organic carbon budget for the York River estuary over the sampling season (June to September 2008) including physical inputs and outputs and biological production and respiration. All values are $\times 10^9$ g C. MPB: microphytobenthos

Allochthonous POC and DOC entering from the watershed and tributaries were found to be comparatively low, accounting for less than 3% of organic carbon inputs during the summer. These allochthonous sources of carbon are likely to be more refractory in nature (McCallister et al. 2004, 2006a,b), which would further limit their bioavailability. The role of MPB in this system also appeared to be limited, contributing only 3% of seasonal organic matter input. While it is likely that some of this organic matter can be transported to the deep channels of the York River following storm events, it is unlikely that this source would contribute significantly to the formation of hypoxia. Future management efforts including nutrient and sediment reduction strategies and improved water clarity may benefit MPB in this system, along with submerged aquatic vegetation, causing these sources to become more significant in the future.

It is interesting to note that the exchanges of POC and DOC to and from the Chesapeake Bay are nearly in balance during the summer. While the net exchange of POC and DOC across the mouth of the estuary appears to currently be in balance, this important exchange should be addressed in future management strategies. Nutrient reduction strategies focused on the tributaries may reduce phytoplankton production in the York River; however, this approach will not reduce POC and DOC entering from the lower Chesapeake Bay. A recent analysis of WC chl *a* concentrations over the past 50 yr by Harding & Perry (1997) found that the lower polyhaline mainstem exhibited the largest increase within any region of the Chesapeake Bay. It is likely that the outcome of nutrient reduction strategies for the York River will be influenced indirectly by the Chesapeake Bay. Similar studies in other sub-estuaries of the Chesapeake Bay have identified the mainstem as a source of labile organic matter, DIN, and DIP (Jordan et al. 1991, Boynton et al. 2008, Testa et al. 2008), which likely contribute to the elevated rates of GPP and net autotrophy in the LYR.

The carbon mass balance indicates that internal water column and benthic respiration is approximately equal to the export of organic matter to the Chesapeake Bay, at 47% and 53% of all loss terms, respectively. Surface (<5 and <9 m for the mesohaline and polyhaline, respectively) water column

respiration in this shallow sub-estuary accounted for the majority of internal aerobic respiration (74%), with sub-pycnocline water column respiration accounting for an additional 15%. Benthic respiration along the shallow shoals and in the deep channels was found to be comparatively low (7% and 4%, respectively) compared to other internal sinks within the estuary. However, these measurements of aerobic respiration likely underestimate total benthic respiration, which includes anaerobic respiration occurring in the deep channel under hypoxic conditions and in anaerobic sediments.

CONCLUSIONS

The oxygen mass balance for the YRE indicates that internal respiration is sufficient to drive the system to hypoxia under stratified conditions, without the need for advection of hypoxic water from the Chesapeake Bay to reproduce the observed declines in DO. Although this system is directly affected by multiple organic matter sources, both autochthonous and allochthonous, this analysis indicates that internal water column phytoplankton production is the dominant source of organic carbon to the YRE during the summer. Reducing this labile source of organic material by implementing nutrient reduction strategies could potentially mitigate some current water quality concerns, although a more complete assessment of the magnitude of nutrient reductions necessary to cause these changes is required over multiple years and under a range of climate scenarios. Additionally, the net exchange of labile organic matter between the lower Chesapeake Bay and the YRE should not be discounted given the potential ecological impacts and associated management implications of these inputs.

Acknowledgements. This project was funded by a grant from NOAA/UNH Cooperative Institute for Coastal and Estuarine Environmental Technology, NOAA Grant Number NA05NOS4191149. S.J. Lake also received financial support from NSF GK-12 (Division of Graduate Education 0840804). We thank Larry Haas, Jennifer Stanhope, Hunter Walker, Lisa Ott, Juliette Giordano, and many other VIMS students and staff members for their field and laboratory assistance. This paper is Contribution No. 3293 of the Virginia Institute of Marine Science, The College of William and Mary.

LITERATURE CITED

Boynton WR, Hagy JD, Cornwell JC, Kemp WM and others (2008) Nutrient budgets and management actions in the Patuxent River estuary, Maryland. Estuaries 31:623–651

Brush MJ (2004) Application of the Greenwich Bay ecosystem model to the development of the Greenwich Bay SAMP (Special Area Management Plan). Final report to the Rhode Island Coastal Resources Center, University of Rhode Island, Narragansett, RI

Buzzelli CP (1998) Dynamic simulation of littoral zone habitats in lower Chesapeake Bay: I. Habitat characterization related to model development. Estuaries 21:659–672

Cartwright GM, Friedrichs CT, Dickhudt PJ, Gass T, Farmer FH (2009) Using the acoustic Doppler velocimeter (ADV) in the MUDBED real-time observing system. In: Marine technology for our future: global and local challenges. Proceedings, OCEANS 2009, MTS/IEEE Biloxi 26–29 Oct (ieeexplore.ieee.org/xpl/mostRecentIssue.jsp?punumber=5412664)

Cloern JE (2001) Our evolving conceptual model of the coastal eutrophication problem. Mar Ecol Prog Ser 210: 223–253

Cooper SR, Brush GS (1991) Long-term history of Chesapeake Bay anoxia. Science 254:992–996

Cooper SR, Brush GS (1993) A 2,500-year history of anoxia and eutrophication in Chesapeake Bay. Estuaries 16: 617–626

Countway RE, Canuel EA, Dickhut RM (2007) Sources of particulate organic matter in surface waters of the York River, VA estuary. Org Geochem 38:365–379

Cowan JL, Boynton WR (1996) Sediment-water oxygen and nutrient exchanges along the longitudinal axis of Chesapeake Bay: seasonal patterns, controlling factors and ecological significance. Estuaries 19:562–580

D'Elia CF, Webb KL, Wetzel RL (1981) Time-varying hydrodynamics and water quality in an estuary. In: Neilson BJ, Cronin LE (eds) Estuaries and nutrients. Humana Press, Clifton, NJ

D'Elia CF, Boynton WR, Sanders JG (2003) A watershed perspective on nutrient enrichment, science, and policy in the Patuxent River, Maryland: 1960-2000. Estuaries 26: 171–185

Dauer DM, Marshall HG, Donat JR, Lane MF, Doughten SC, Morton PL, Hoffman FA (2005) Status and trends in water quality and living resources in the Virginia Chesapeake Bay: James River (1985-2004). Final Report to the Virginia Department of Environmental Quality, Richmond, Virginia. Applied Marine Research Laboratory, Norfolk, VA

de Jonge VN (1997) High remaining productivity in the Dutch western Wadden Sea despite decreasing nutrient inputs from riverine sources. Mar Pollut Bull 34:427–436

de Jonge VN, van Beusekom JEE (1995) Wind- and tide-induced resuspension of sediment and microphytobenthos from tidal flats in the Ems Estuary. Limnol Oceanogr 40:766–778

Diaz RJ, Rosenberg R (1995) Marine benthic hypoxia: a review of its ecological effects and the behavioural responses of benthic macrofauna. Oceanogr Mar Biol Annu Rev 33:245–303

Diaz RJ, Rosenberg R (2008) Spreading dead zones and consequences for marine ecosystems. Science 321:926–929

Diaz RJ, Neubauer RJ, Schaffner LC, Pihl L, Baden SP (1992) Continuous monitoring of dissolved oxygen in an estuary experiencing periodic hypoxia and the effects of hypoxia on macrobenthos and fish. Sci Total Environ (Suppl 1992):1055–1068

Fisher TR, Hagy JD, Boynton WR, Williams MR (2006) Cultural eutrophication in the Choptank and Patuxent Estu-

aries of Chesapeake Bay. Limnol Oceanogr 51:435–447
Giordano JCP (2009) Nutrient loading and system response in the coastal lagoons of the Delmarva Peninsula. Masters thesis, College of William and Mary, Virginia Institute of Marine Science, Gloucester Point, VA
Giordano JCP, Brush MJ, Anderson IC (2012) Ecosystem metabolism in shallow coastal lagoons: patterns and partitioning of planktonic, benthic, and integrated community rates. Mar Ecol Prog Ser 458:21–38
Haas LW (1977) The effect of the spring-neap tidal cycle on the vertical salinity structure of the James, York, and Rappahannock Rivers, Virginia, USA. Est Coast Mar Sci 5:485–496
Haas LW, Hastings SJ, Webb KL (1981) Phytoplankton response to a stratification-mixing cycle in the York River estuary during late summer. In: Neilson BJ, Cronin LE (eds) Estuaries and nutrients. Humana Press, Clifton, NJ
Hagy JD, Boynton WR, Keefe CW, Wood KV (2004) Hypoxia in Chesapeake Bay, 1950–2001: long-term changes in relation to nutrient loading and river flow. Estuaries 27: 634–658
Harding LW Jr, Perry ES (1997) Long-term increase of phytoplankton biomass in Chesapeake Bay, 1950–1994. Mar Ecol Prog Ser 157:39–52
Harding LW Jr, Mallonee ME, Perry ES (2002) Toward a predictive understanding of primary productivity in a temperate, partially stratified estuary. Estuar Coast Shelf Sci 55:437–463
Hayward D, Welch CS, Haas LW (1982) York River destratification: an estuary-subestuary interaction. Science 216: 1413–1414
Hayward D, Haas LW, Boon JD III, Webb KL, Friedland KD (1986). Empirical models of stratification variation in the York River estuary, Virginia, USA. In: Bowman MJ, Yentsch CM, Peterson WT (eds) Lecture notes on coastal and estuarine studies: tidal mixing and plankton dynamics. Springer-Verlag, New York, NY
Jassby AD, Platt T (1976) Mathematical formulations of the relationship between photosynthesis and light for phytoplankton. Limnol Oceanogr 21:540–547
Jordan TE, Correll DL, Miklas J, Weller DE (1991) Long-term trends in estuarine nutrients and chlorophyll, and short-term effects of variation in watershed discharge. Mar Ecol Prog Ser 75:121–132
Kemp WM, Boynton WR (1980) Influence of biological and physical processes on dissolved oxygen dynamics in an estuarine system: implications for measurement of community metabolism. Estuar Coast Mar Sci 11:407–431
Kemp WM, Sampou PA, Garber J, Tuttle J, Boynton WR (1992) Seasonal depletion of oxygen from bottom waters of Chesapeake Bay: roles of benthic and planktonic respiration and physical exchange processes. Mar Ecol Prog Ser 85:137–152
Kemp WM, Smith EM, Marvin-DiPasquale M, Boynton WR (1997) Organic carbon balance and net ecosystem metabolism in Chesapeake Bay. Mar Ecol Prog Ser 150: 229–248
Kemp WM, Puskaric S, Faganeli A, Smith E, Boynton W (1999) Pelagic-benthic coupling and nutrient cycling. In: Malone T, Malej A, Harding L, Smodlaka N, Turner R (eds) Ecosystems at the land-sea margin: drainage basin to coastal sea. American Geophysical Union, Washington, DC
Kemp WM, Boynton WR, Adolf JE, Boesch DF and others (2005) Eutrophication of Chesapeake Bay: historical trends and ecological interactions. Mar Ecol Prog Ser 303:1–29
Kuo AY, Neilson BJ (1987) Hypoxia and salinity in Virginia estuaries. Estuaries 10:277–283
Kuo AY, Neilson BJ, Brubaker J, Ruzecki EP (1993) Hypoxia in the York River, 1991. Virginia Institute of Marine Science Data Report No. 47. Gloucester Point, VA
Lake SJ, Brush MJ (2011) The contribution of microphytobenthos to total productivity in Narragansett Bay, Rhode Island. Estuar Coast Shelf Sci 95:289–297
Laws EA (1991) Photosynthetic quotients, new production and net community production in the open ocean. Deep-Sea Res 38:143–167
Lehrter JC, Cebrian J (2010) Uncertainty propagation in an ecosystem nutrient budget. Ecol Appl 20:508–524
Lorenzen C (1967) Determination of chlorophyll and phaeopigments: spectrophotometric equations. Limnol Oceanogr 12:343–346
Malone TC, Kemp WM, Ducklow HW, Boynton WR, Tuttle JH, Jonas RB (1986) Lateral variation in the production and fate of phytoplankton in a partially stratified estuary. Mar Ecol Prog Ser 32:149–160
McCallister SL, Bauer JE, Cherrier JE, Ducklow HW (2004) Assessing sources and ages of organic matter supporting river and estuarine bacterial production: a multiple-isotope approach. Limnol Oceanogr 49:1687–1702
McCallister SL, Bauer JE, Canuel EA (2006a) Bioreactivity of estuarine dissolved organic matter: a combined geochemical and microbiological approach. Limnol Oceanogr 51:94–100
McCallister SL, Bauer JE, Ducklow HW, Canuel EA (2006b) Sources of estuarine dissolved and particulate matter: a multi-tracer approach. Org Geochem 37:454–468
Møhlenberg F (1999) Effect of meteorology and nutrient load on oxygen depletion in a Danish micro-tidal estuary. Aquat Ecol 33:55–64
Neubauer SC, Anderson IC (2003) Transport of dissolved inorganic carbon from a tidal freshwater marsh to the York River estuary. Limnol Oceanogr 48:299–307
Officer CB (1980) Box models revisited. In: Hamilton P, MacDonald KB (eds) Estuarine and wetland processes with emphasis on modeling. Plenum Press, New York, NY
Officer CB, Biggs RB, Taft JL, Cronin LE, Tyler MA (1984) Chesapeake Bay anoxia: origin, development, and significance. Science 223:22–27
Paerl HW, Pinckney JL, Fear JM, Peierls BL (1998) Ecosystem responses to internal and watershed organic matter loading: consequences for hypoxia in the eutrophying Neuse River estuary, North Carolina, USA. Mar Ecol Prog Ser 166:17–25
Pemberton M, Anderson GL, Barker JH (1996) Characterization of microvascular vasoconstriction following ischemia/reperfusion in skeletal muscle using video-microscopy. Microsurgery 17:9–16
Pinckney JL, Zingmark RG (1993) Modeling the annual production of intertidal benthic microalgae in estuarine ecosystems. J Phycol 29:396–407
Platt T, Gallegos CL, Harrison WG (1980) Photoinhibition of photosynthesis in natural assemblages of marine phytoplankton. J Mar Res 38:687–701
Rabalais NN, Turner RE, Gupta BKS, Boesch DF, Chapman P, Murrell MC (2007) Hypoxia in the northern Gulf of Mexico: does the science support the plan to reduce, mitigate and control hypoxia? Estuaries 30:753–772

Raymond PA, Bauer JE (2000) Bacterial consumption of DOC during transport through a temperate estuary. Aquat Microb Ecol 22:1–12

Reay WG, Gallagherl DL, Simmons GM Jr (1995) Sediment-water column oxygen and nutrient fluxes in nearshore environments of the lower Delmarva Peninsula, USA. Mar Ecol Prog Ser 118:215–227

Seliger HH, Boggs JA, Buggley WH (1985) Catastrophic anoxia in the Chesapeake Bay in 1984. Science 228: 70–73

Sharples J, Simpson JH, Brubaker JM (1994) Observations and modelling of periodic stratification in the upper York River estuary, Virginia. Estuar Coast Shelf Sci 38:301–312

Shen J, Haas L (2004) Calculating age and residence time in the tidal York River using three-dimensional model experiments. Estuar Coast Shelf Sci 61:449–461

Shoaf WT, Lium BW (1976) Improved extraction of chlorophyll *a* and *b* from algae using dimethyl sulfoxide. Limnol Oceanogr 21:926–928

Smith EM, Kemp WM (1995) Seasonal and regional variations in plankton community production and respiration for Chesapeake Bay. Mar Ecol Prog Ser 116:217–231

Smith EM, Kemp WM (2003) Planktonic and bacterial respiration along an estuarine gradient: responses to carbon and nutrient enrichment. Aquat Microb Ecol 30:251–261

Taft JL, Hartwig EO, Loftus R (1980) Seasonal oxygen depletion in Chesapeake Bay. Estuaries 3:242–247

Testa JM, Kemp WM (2008) Variability of biogeochemical processes and physical transport in a partially stratified estuary: a box-modeling analysis. Mar Ecol Prog Ser 356: 63–79

Testa JM, Kemp WM, Boynton WR, Hagy JD III (2008) Long-term changes in water quality and productivity in the Patuxent River estuary: 1985–2003. Estuaries 31:1021–1037

Editorial responsibility: William Kemp, Cambridge, Maryland, USA

Submitted: June 5, 2012; Accepted: July 2, 2013
Proofs received from author(s): October 1, 2013